REPORT DOCUMENTATION PAGE

Form Approved
OMB No. 0704-0188

PLEASE DO NOT RETURN YOUR FORM TO THE ABOVE ADDRESS.

1. REPORT DATE *(DD-MM-YYYY)*	2. REPORT TYPE	3. DATES COVERED *(From - To)*
03-30-2009	Final	Sep 2006 - Sep 2008

4. TITLE AND SUBTITLE
NRL/NAVSEA Research and Related

5a. CONTRACT NUMBER
N00173-06-2-C008

5b. GRANT NUMBER

5c. PROGRAM ELEMENT NUMBER

6. AUTHOR(S)
Thames, Shelby, F
Rawlins, James, W
Mathias, Lon
Mauritz, Kenneth
Nazarenko, Sergei
Storey, Robson, F
Urban, Marek

5d. PROJECT NUMBER
61-0373-06

5e. TASK NUMBER

5f. WORK UNIT NUMBER

7. PERFORMING ORGANIZATION NAME(S) AND ADDRESS(ES)
The University of Southern Mississippi
118 College Drive #5157
Hattiesburg, MS 39406-0001

8. PERFORMING ORGANIZATION REPORT NUMBER
GR02764...

9. SPONSORING/MONITORING AGENCY NAME(S) AND ADDRESS(ES)
Kevin M. King
4555 Overlook Avenue, S.W.
Washington, DC 20375-5326
202-767-1495; kevin.king@nrl.navy.mil

10. SPONSOR/MONITOR'S ACRONYM(S)
3220.KK

11. SPONSOR/MONITOR'S REPORT NUMBER(S)

12. DISTRIBUTION/AVAILABILITY STATEMENT
For public distribution

13. SUPPLEMENTARY NOTES

14. ABSTRACT

(1) Waterborne, very low volatile organic compound (VOC) content Navy haze gray (NHG) coatings were developed using vegetable oil macromonomer (VOMM)-based latexes. The coatings successfully met the requirements of specifications MIL-PRF-24635C and MIL-PRF-24569A. The monomer and latex syntheses were scaled up to prepare 20 gallons of the NHG coating, which was shipped to two Florida locations, Pentech and NRL, for evaluation on December 2, 2008. AFM characterization techniques developed to track film coalescence as a function of drying time indicated that the coalescence rate increased with increasing VOMM content. (2) BoltornTM dendritic hydroxylated esters were evaluated as high oxygen barrier biodegradable films and coatings. Improved mechanical performance was achieved via covalent linking of dendritic molecules with 1,6-hexamethylene diisocyanate. (3) Biodegradable thermoplastic polyurethane (TPU) elastomers were synthesized using poly (D,L-lactide-co-glycolide) polyesters, poly(butylene adipate), dicyclohexylmethane-4,4'-diisocyanate, and 1,4-butanediol, and evaluated for the performance properties and degradability in sea water. The unique properties of these TPUs make them attractive

15. SUBJECT TERMS
Navy haze gray coating, oxygen barrier coatings, biodegradable coatings, thermoplastic polyurethane elastomers, nanocomposites

16. SECURITY CLASSIFICATION OF:			17. LIMITATION OF ABSTRACT	18. NUMBER OF PAGES	19a. NAME OF RESPONSIBLE PERSON
a. REPORT	b. ABSTRACT	c. THIS PAGE			Drs. James Rawlins and Shelby Thames
UU	UU	UU	UU	26	19b. TELEPHONE NUMBER *(Include area code)* 601-266-5618

NRL/NAVSEA RESEARCH AND RELATED
Final Report
Naval Research Laboratory

Award No. N00173-06-2-C008

Period of Performance 09/30/06 through 09/29/2008

Drs. James Rawlins and Shelby Thames
The University of Southern Mississippi
School of Polymers and High Performance Materials
118 College Drive #10037
Hattiesburg, MS 39406-0001

March 31, 2009

ENVIRONMENTALLY FRIENDLY LOW-NO VOC NAVY HAZE GRAY (NHG) COATINGS

PIs: Shelby F. Thames and James W. Rawlins

Navy Haze Gray Coating

Introduction

Naval ships require speeialized eoatings to eombat the severely corrosive marine environments. Naval coatings that eome into eontaet with seawater possess anti-fouling properties to prevent fouling deposits from aecumulating on the ship's surface. On the other hand, exterior coatings sueh as Navy Haze Gray that are applied to the topside of ships form an integral componcnt of the ship's counter-measures weapons system. Apart from proteeting topside meehanical equipment and structures from the weather, these coatings also provide visual eamouflage by blending the ship into the open oeean baekground.

Current Navy Haze Gray coatings are formulated from solvent-based silicone-modified alkyds that contain high amounts of volatile organic compounds (VOCs). For example, Interlac 2 supplied by International Marine Coatings has VOC levels of 336 g/L (2.80 lb/gal) at 60± 2% volume solids and a flash point of 100°F (Setaflash). Interlae 2 has a touch-dry time of 2 hours and hard-dry time of 8 hours at 77°F and meets MIL specification MIL-PRF-24635B (SH) LSA TYII CL2. Therefore, our research objective is to develop an environmentally-friendly waterborne eoating with minimal odor and low-to-zero VOC eontent. Waterborne coatings offer the additional advantages of ease of elean-up, redueed fire hazards, and low toxieity to Navy personnel.

The Thames-Rawlins Research Group (TRRG) is engaged in researeh and development of environmentally friendly produets sueh as formaldehyde-free eomposites, and eosolvent-free latexes to reduce the nation's relianee on petroleum derivatives. A novel class of vegetable oil macromonomers (VOMMs) were designed and developed to synthesize eosolvent-free latexes. VOMMs contain three separate and identifiable functionalities. First, the acrylic moiety through which free-radical initiated polymerizations ean proeeed; seeondly, the C18 flexible hydrocarbon ehain that functions as a powerful coalescing aid; and finally, the CH_2 flanked 9-10 olefinie double bond via whieh oxidative polymerization oecurs. In practice, the acrylate functionality allows for facile eopolymerization of the VOMM with eommon monomers such as vinyl aeetate, methyl methacrylate, methyl acrylate, butyl acrylate, styrene, and many more. Sinee the VOMM is copolymerized into the polymer baekbone, it is non-fugitive and consequently odor free, non-VOC, and friendly to the environment.

Monomer Synthesis

A 1000 mL three-neck flask equipped with a thermoeouple, eondenser, mechanical stirrer, and nitrogen purge was charged with 500.0 g soybean oil. Nitrogen was bubbled through the oil for 12 hours. The oil was then heated to 60°C and sodium methoxide catalyst was added followed by *N*-methyl ethanolamine. The reaction was monitored via Fourier Transform-Infrared (FT-IR)

spectroscopy by following the disappearance of the ester peak and appearance of the amide peak. The product was then washed with brine solution to remove glycerol and excess *N*-methyl ethanolamine. After washing, the fatty amide product was dried with magnesium sulfate and filtered, and characterized by GPC (gel permeation chromatography) and NMR (nuclear magnetic resonance).

A 500 mL three-neck flask equipped with mechanical stirrer, addition funnel, and temperature probe was charged with 250 g of the above fatty amide, 0.01 molar excess triethylamine (based on fatty amide equivalent weight), and 100 g methylene chloride. The flask was cooled to 0°C, and acryloyl chloride was added dropwise over 2 hours. The product was washed with brine solution to remove hydrochloric acid and other impurities, dried with magnesium sulfate, and the solvent removed by vacuum distillation. The product (SoyAA-1) was characterized by GPC, HPLC (High Performance Liquid Chromatography), gas chromatography (GC), and NMR.

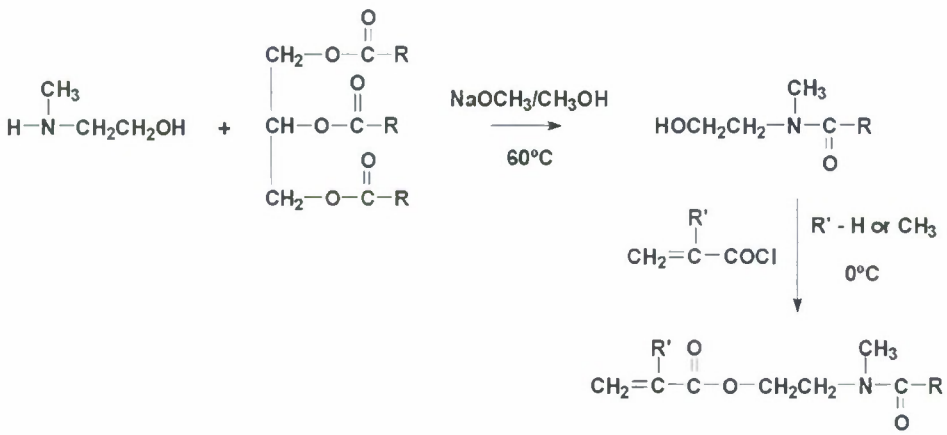

Figure 1. Soybean oil macromonomer synthesis.

Latex Synthesis

Latexes containing 40 wt% of SoyAA-1 were synthesized in 1000 mL glass reaction kettles using a seeded, semi-continuous method in which both monomer and initiator were introduced into the reactor at a controlled rate using a Camile® 2000 automated data acquisition and control system. Manually programmed syringe pumps were used to control initiator feed rate. The reaction temperature was controlled by partially submerging the reaction vessel in a water bath regulated at a constant temperature with an immersion circulator. A Claisen adapter was utilized to mount a nitrogen inlet and condenser. The remaining kettle lid openings were sealed with rubber septa. Initiator solutions and monomers were introduced into the reactor through needles placed in the septa, taking care to separate the needle tips.

Navy Haze Gray Coating

The Navy Haze Gray coating requires a blend of pigments to achieve the gray shade listed in the MIL specifications. The specific pigments employed in this formulation are designed to meet the

Navy's requirements of low detectability. To minimize flocculation issues, the pigments were co-dispersed in a tint base (Table 1).

Table 1. Mill Base Formulations

Colored Tint Base	
Water	117.05
Disperbyk® 182	29.91
BYK® 021	3.22
Kathon® LX 1.5%	0.32
AMP-95	0.32
Aerosil® 200	0.73
Red iron oxide	68.00
Yellow iron oxide	79.20
Phthalocyanine blue	18.89

After the tint bases were dispersed to a Hegman gauge of 7+, they were formulated into the Navy Haze Gray coating as shown in Table 2.

Table 2. Navy Haze Gray Coating

Water	5.19
Tamol® 731A	0.11
Natrosol® Plus 330	0.03
Ammonium hydroxide	0.06
Triton® CF-10	0.04
BYK 022	0.02
Ti-Pure® R-706	5.55
Huber® 70C	5.55
Colored tint base	0.95
Water	0.67
Surfynol® 104A	0.10
Acrysol™ RM 2020 NPR	2.07
VOMM latex	77.05
Optifilm® Enhancer 400	1.26
Tinuvin® 5151	0.70
Cobalt Hydrocure® II	0.65
Total	100.00

The coating viscosity was adjusted to 83-87 Krebs Units at 25°C by adjusting the amount of rheology modifier (Acrysol RM 2020 NPR). The cosolvent (Optifilm Enhancer 400) and UV absorber package (Tinuvin 5151) were premixed to ensure complete dissolution of Tinuvin 5151.

The coatings were tested for compliance with MIL-PRF-24635C and MIL-PRF-24569A (Tables 3 and 4).

Table 3. Testing Results per MIL-PRF-24635C Generation 6 Coating

Test Number	Description	Generation 6	Requirement
4.6.1	Pigment, weight %	10.59%	As specified by manufacturer
	Volatile weight %	46.94	
	Mass per unit volume	1.125	
	Viscosity	84.3 KU	< 100 KU
	Specular gloss @ 60°	58.4	45-60
	Hiding power (contrast ratio)	100.0	> 90
4.6.1.2	Adhesion	Pass	Pass
4.6.2	Pot life	Not applicable	Not applicable
4.6.3	Drying time (minutes) @ 72 °F		
4.6.3 4.6.3.1	Set-to-touch	9	< 120
	Dust free	10	< 120
	Dry through	13	< 480
	Dry hard	14	< 480
	Full hardness	7 days	
4.6.4	Volatile organic compound (VOC)	< 15 g/L	< 275 g/L
4.6.4.1	Class 3 submarine atmosphere volatiles	Classified	Classified
4.6.5	HAP content of coatings	None	< 0.5-1.0
4.6.6	Hazardous pigments and additives	None	< 5 mg/l
4.6.6.1	Tantalum and tungsten content	None	< 0.100
4.6.7	Yellowness (1 year)	In progress	< 3.0
4.6.8	Mixing properties	Pass	Pass
4.6.9	Spraying properties	Pass	Pass
4.6.10	Brushing properties	Pass	Pass
4.6.11	Flexibility	Pass	Pass
4.6.12	Knife test	Pass	Pass
4.6.13	Water resistance	Not applicable	Not applicable
4.6.14	Hydrocarbon fluid resistance	Not applicable	Not applicable
4.6.15	Salt spray resistance	Pass	Pass
4.6.16	Condensation blister resistance	None	# 8 few
4.6.17	Exudate formation	Pass	Pass
4.6.18	Washability	63%	> 50% gloss retention
	Flash rust resistance	Pass	Pass
4.6.19	Recoatability	In progress	Pass
4.6.20	Radiant panel test	Tests to be performed by NRL	
4.6.21.2	Smoke density chamber test		
4.6.21.3	Resistance to ignition		
4.6.21.4	Flashover determination		
4.6.21.5	Heat transfer		

Table 4. Coatings Test Results per MIL-PRF-24569A for Generation 6 Coating

Test number	Description	Generation 6	Requirement
4.6.1	Condition in container	Pass	Pass
4.6.2.1	Partially full container	In progress	Pass
4.6.2.2	Full container	In progress	Pass
4.6.2.3	Accelerated storage stability	Pass	Pass
4.6.3	Dilution stability	Pass	Pass
4.6.4	Brushing properties	Pass	Pass
4.6.5	Rolling properties	Pass	Pass
4.6.6	Spraying properties	Pass	Pass
4.6.7	Color		
	L*	56.12	56.0 ± 0.3
	a*	-1.51	-1.56 ± 0.3
	b*	-1.46	-1.37 ± 0.3
4.6.8	Odor	Slight solvent odor	Not obnoxious or objectionable
4.6.9	Anchorage	Pass	Pass
4.6.10	Flexibility	Pass	Pass
4.6.11	Flake and crack resistance	Pass	Pass
4.6.12	Enamel recoatability	In progress	Pass
4.6.13	Water resistance	No blistering	No blistering
4.6.14	Vehicle extraction	Not applicable*	Not applicable*
4.6.15	Silicone-alkyd copolymer resin	Not applicable*	Not applicable*
4.6.16	Specular gloss @ 60°	58.4	45-60
4.6.17	Drying time (minutes) @ 72 °F		
	Set-to-touch	9	< 120
	Dust free	10	< 120
	Dry through	13	< 480
	Dry hard	14	< 480
4.6.18	Accelerated weathering (300 hours QUV)		
	Δ L*	0.23	≤ 1.0
	Δ a*	0.71	≤ 1.0
	Δ b*	0.14	≤ 1.0
	Gloss change @ 60°	13%	≤ 35%
4.6.19	Volatile organic compound (VOC)	< 15 g/L	< 275 g/L
4.6.20	Soluble and total metal content	Not applicable*	Not applicable
4.6.20.1	Tantalum and tungsten content	Not applicable*	Not applicable*
4.6.21	Long term exterior exposure	In progress	Pass
4.6.22	Flash point	Not applicable*	Not applicable*
	Water content	Not applicable*	Not applicable*
	Coarse particles	< 0.5	< 0.5

	Consisteney	84.3 KU	< 100 KU
	Fineness of grind	7+	6+
	Contrast ratio	100.0	> 90
4.6.23	Hazardous solvent content	None added	0.05-0.1 maximum

Tables 3 and 4 demonstrate that the soybean oil maeromonomer-based Navy Haze Gray coating successfully met the requirements of the two MIL specifieations. The monomer and latex synthcses were then sealed up to manufacture 20 gallons of the eoating. As recommended by Dr. Keith E. Lueas, Director, Center for Corrosion Seience and Engineering, via his letter dated Sep 3, 2008 (Ref: 5700 Ser 6130-356) (sce Appendix A), we shipped 10 gallons of the coating to each of thc following addresses for their evaluation on Deeember 2, 2008:

1) Mr. Tom Pennell
Pentech, Inc.
7256 21st Street East
Sarasota, FL 34243

2) Mr. Ivan Stanke
Bldg F-14, Fleming Key
Trumbo Point Annex
Key West, FL 33040

We are waiting for their evaluation results. Upon their approval, the eoatings will be ready for evaluation aboard naval ships.

Patents

"Glycerol Ester-Free Vegetable Oil Derivatives," Shelby F. Thames, James W. Rawlins, David Dclattc, and Sharathkumar K. Mendon, applieation filed January 2007, USM:087.

APPENDIX A

DEPARTMENT OF THE NAVY
NAVAL RESEARCH LABORATORY
4555 OVERLOOK AVE SW
WASHINGTON DC 20375-5320

IN REPLY REFER TO
5700
Ser 6130-356
September 3, 2008

James Rawlins, Ph.D.
University of Southern Mississippi
118 College Drive #10037
Hattiesburg, MS 39406-0001

Dear Dr. Rawlins:

SUBJ: FUTURE NAVAL CAPABILITIES, ACQUISITION OF ADVANCED TOPSIDE COATING SYSTEM FOR PANEL TESTING

1. The purpose of this letter is to inform you that the Naval Research Laboratory (NRL) has identified your product as a potential candidate for use as a topside coating system. The products coating properties are favorable relative to currently qualified products and NRL would like to include your product in our Future Naval Capabilities effort for Advanced Topside Coating Systems.

2. To begin the evaluation process NRL would like a quotation from USM to provide 20 gallons of product packaged in one gallon cans for initial screening tests. If the product has a specially formulated primer, please include it in your quotation.

3. The screening tests will consist of the following from MIL-PRF-24635D, unless otherwise stated:

- Xenon-arc, ASTM G155
- Accelerated weathering, section 3.5.23/4.5.23
- Long-term exterior exposure, section 3.5.25/4.5.25
- Edge retention, MIL-PRF-23236C section 3.8.1/4.5.9 (Appendix A)
- Color, section 3.5.16/4.5.16
- Gloss, section 3.5.17/4.5.17

5700
Ser 6130-356
September 3, 2008

4. When submitting the material include the necessary material safety data sheets, product data sheets, and ensure that all submitted material is from the same batch. Container labeling shall be as follows: [FNCTopside/USM/Can #/Component]. If you are unable to provide the required material please state your reasoning and NRL will try to accommodate within reason.

5. When shipping please prepare two shipments and send 10 gallons of material to each of the following addresses:

Attn: Tom Pennell	Attn: Ivan Stanke
Pentech, Inc.	Bldg F-14, Fleming Key
7256 21st Street East	Trumbo Point Annex
Sarasota, FL 34243	Key West, FL 33040
Phone: 941-739-2700	Phone: 305-293-4214

6. If these screening tests support the original claims and meet the original objectives provided in the RFI a more detailed testing evaluation effort may result.

7. The primary points of contact are Ted Lemieux, NRL Code 6136, at 305-293-4214 or email to edward.lemieux@nrl.navy.mil; Dr. Airan J. Perez, Office of Naval Research, email to airan.perez@navy.mil.

Keith E. Lucas
Director, Center for Corrosion
Science and Engineering

NAVY HAZE GRAY FILM CHARACTERIZATION

PI: Dr. Marek Urban

As latexes are analytically complex systems, Raman band assignments cannot be taken directly from databases. Therefore, reference compounds were used to determine the bands that represented specific functional groups in the latex.

Figures 1A and 1B show Raman spectra of a control latex (formulated with butyl acrylate and methyl methacrylate) and a vegetable oil macromonomer (VOMM)-based latex (formulated with butyl acrylate, methyl methacrylate, and SoyAA-1). The latex spectra is quite complex and no *significant* differences can be resolved with Raman spectroscopy at this stage.

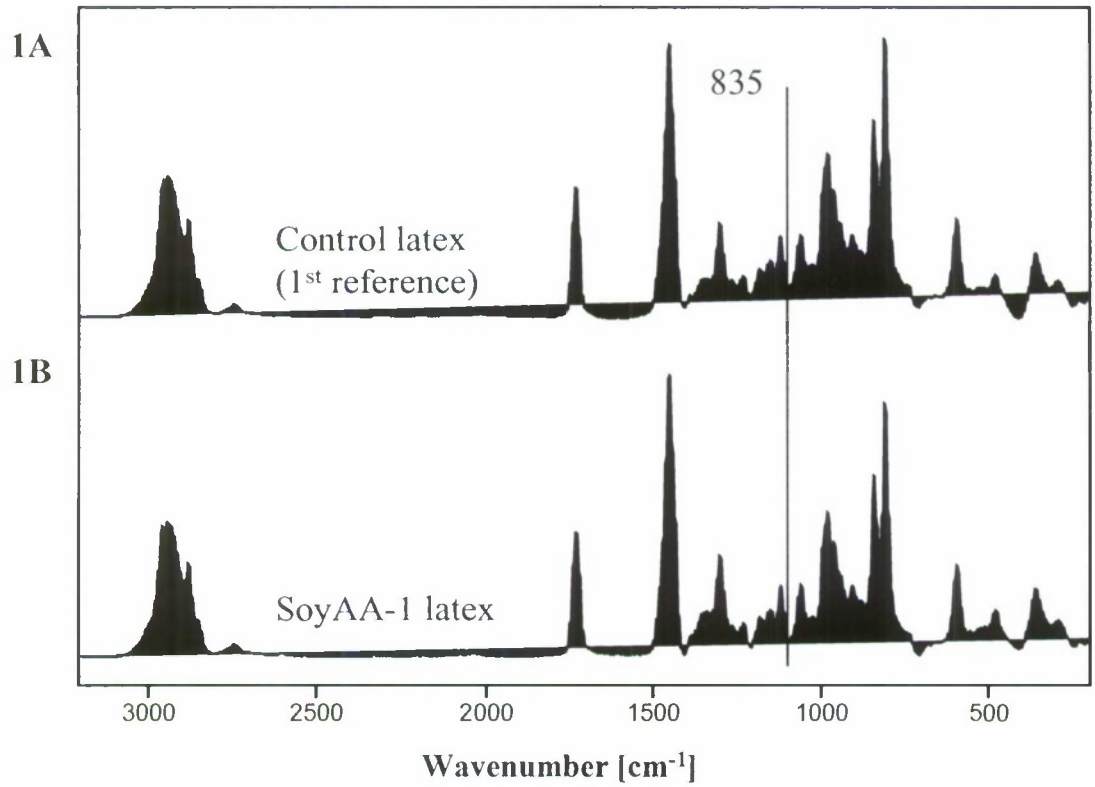

Figure 1. Raman spectra of control and SoyAA-1 latexes.

Figure 2 compares the Raman spectra of SoyAA-1 monomer and SoyAA-1 latex films that were dried at ambient for 24 hours. Figures 2A and 2B both exhibit a strong band at 1655 cm^{-1} (-C=O). This band does not appear in Figure 1B, i.e., the soy latex *before* exposure to atmosphere. Moreover, the band at 835 cm^{-1} (-C=C-) is seen to diminish significantly from spectra 1B to 2B, indicating that the vegetable oil unsaturation is almost completely consumed upon atmospheric exposure.

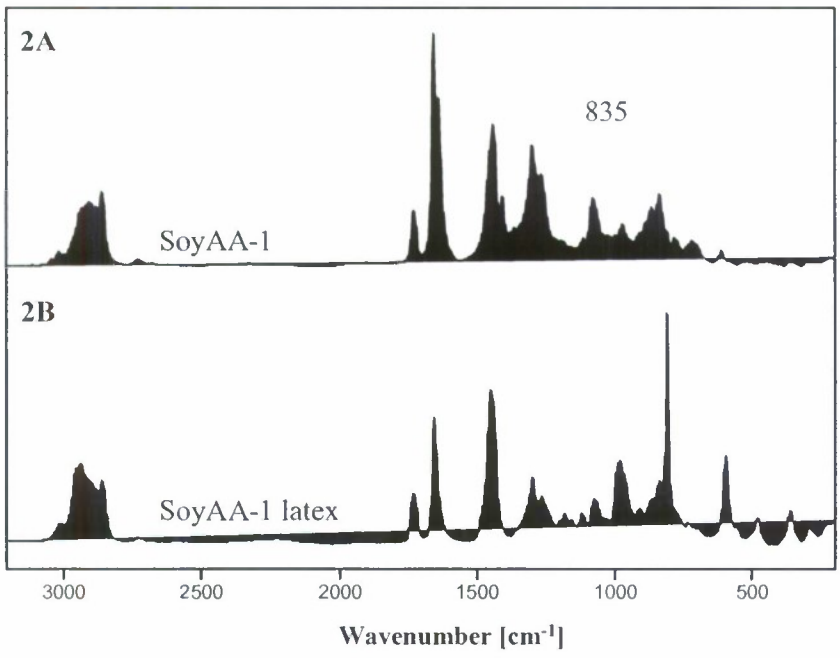

Figure 2. Raman spectra of SoyAA-1 and SoyAA-1 latex after exposure for 24 hours at ambient.

Figure 3 shows the Raman spectra of SoyAA-1 latexes obtained as a function of drying time. It is seen that the band at 1635 cm^{-1} stayed constant within the timeframe of 24 hours (3A) to 144 hours (3C). These three spectra suggest that the SoyAA-1 latex reacts with atmospheric oxygen primarily within the first 24 hours of exposure.

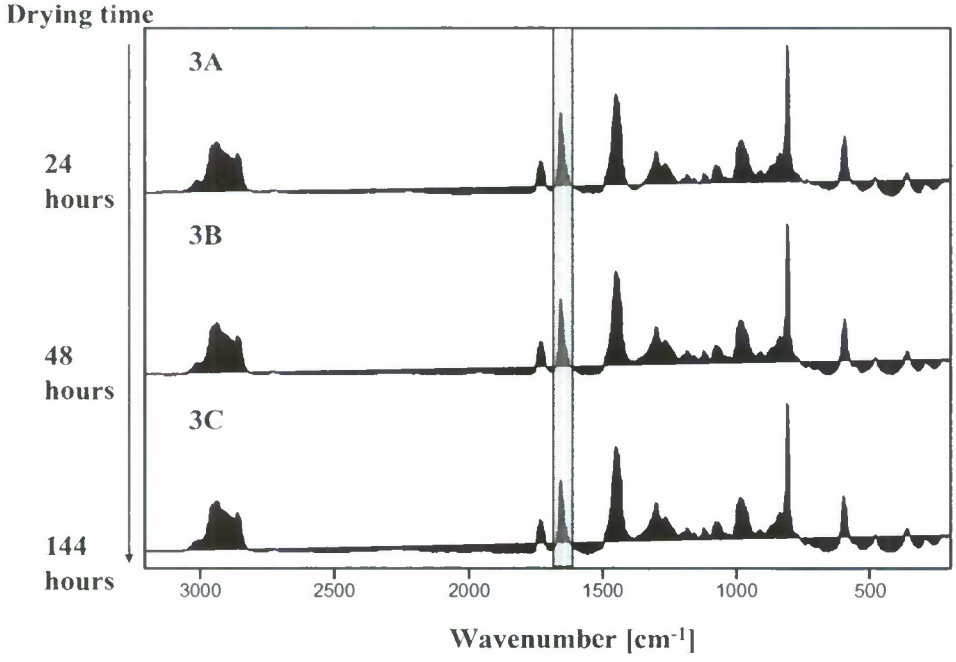

Figure 3. Raman spectra of SoyAA-1 latex as a function of drying time.

NAVSEA AFM CHARACTERIZATION

PI: Sarah E. Morgan

Objective

1) To provide AFM characterization of environmentally-friendly Navy Haze Gray (NHG) coatings based on vegetable oil macromonomers (VOMM) in Thames-Rawlins Research Group for optimizing coatings formulations
2) To enhance surface analysis capability through acquisition of a lab scale tribometer

Summary

AFM characterization techniques were developed to track film coalescence as a function of drying time, and indicated that coalescence rate increased with increasing VOMM content. A MicroPhotonics pin-on-disk tribometer was acquired and installed. This research resulted in one preprint[1] and another manuscript is in preparation.

VOMM Coatings Characterization

Introduction

Atomic force microscopy (AFM) is a powerful technique for imaging surfaces of soft samples such as polymeric systems without the need for extensive sample preparation or staining, and with minimal damage to the sample. This allows other complementary analyses to be performed on a single sample. Surface morphology of composite surfaces and/or fracture surfaces is readily imaged in tapping mode AFM. Similarly, thin films of varying compositions can be prepared via different techniques to evaluate their surface morphology. Tip-sample forces, evaluated via force curves, provide information about the surface hardness and modulus, as well as adhesion between the probe and the surface.

Experimental

Surfaces of VOMM films were examined using tapping mode AFM using a Dimension 3000 AFM (Digital Instruments, Santa Barbara, CA) to obtain height and phase images. Images were collected in tapping mode using a 125 μm long etched silicon probe with a resonant frequency of 275 kHz, nominal force constant of 40 N/m, and a nominal tip radius of 10 nm. Multiple areas were imaged and representative images are reported.

Results and Discussion

Coalescence rate increased as a function of VOMM concentration for films dried at ambient temperature. Figure 1 shows tapping mode images of formulations with 20% (a), 40% (b) and 60% (c) VOMM concentration after one day of drying. While distinct particles are clearly observed in the 20% sample, particles are diffuse in the 40% sample and it is difficult to distinguish particles in the 60% sample, indicating complete film coalescence. Measured root

mean square roughness (RMS) decreased with increasing VOMM content, indicating improved film coalescence.

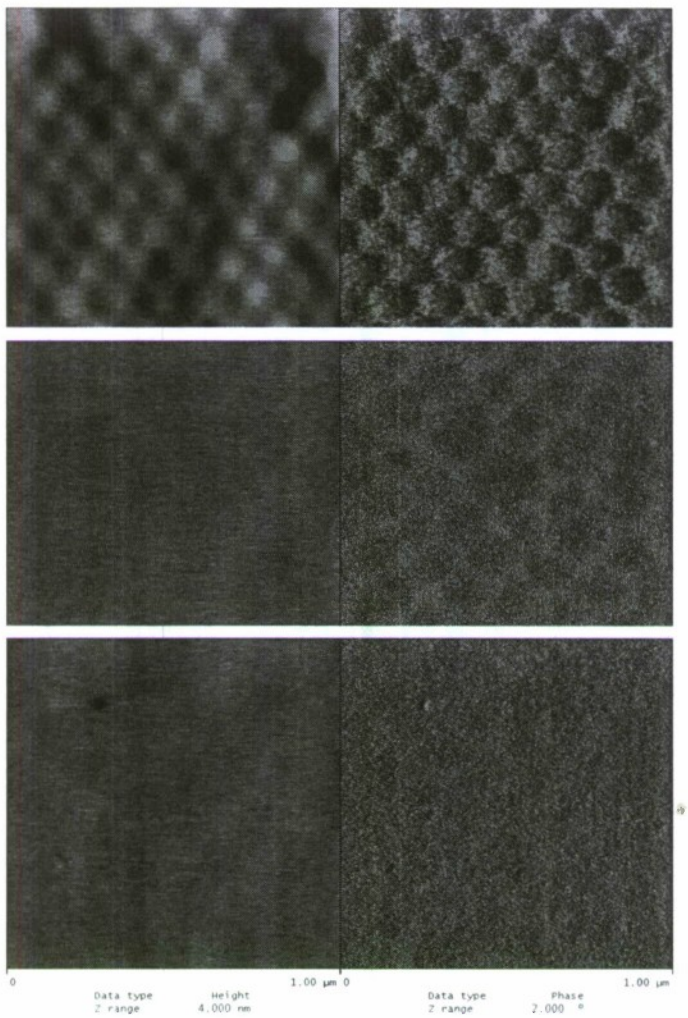

Figure 1. AFM height and phase image for films containing 20% (a), 40% (b) and 60% (c) VOMM after one day of drying. RMS Roughness: a) 1.1 nm b) 0.35 nm c) 0.28 nm

Figure 2 shows AFM images for the same samples after 11 days. While the 20% VOMM sample still exhibited non-coalesced particles, the 40% and 60% samples appear completely smooth. RMS roughness values indicate enhanced coalescence for the higher VOMM content samples.

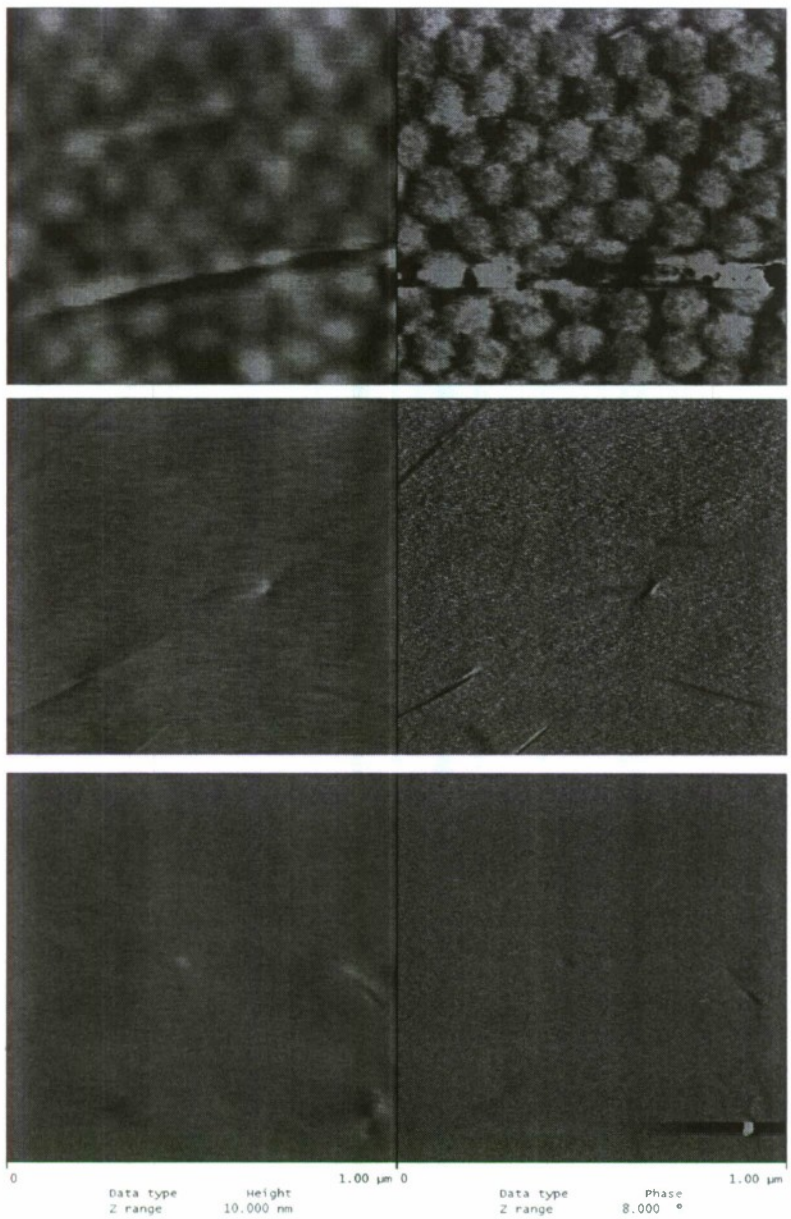

Figure 2. AFM height and phase image for films containing 20% (a), 40% (b) and 60% (c) VOMM after 11 days of drying. RMS Roughness: a) 1.1 nm, b) 0.28 nm, c) 0.37 nm

Conclusions

AFM imaging is useful for determining film coalescence rates. Coatings containing high levels of VOMM show rapid film coalescence at ambient temperature, indicating design flexibility in incorporation of VOMM in environmentally friendly coatings.

Friction Performance of Polyhedral Oligomeric Silsesquioxane (POSS) Nanocomposites

Introduction

POSS molecules consist of an Si-O-Si inorganic cage surrounded by an organic corona.[2] The diameter of these monodisperse particles ranges from one to three nanometers, depending on the composition of the cage.[3] Surface properties of POSS-based high performance nanocomposites (HPNCs) can be tailored by varying the substituent organic group attached to the inorganic cage while maintaining the bulk properties of the neat polymer. Recently, we reported significant reduction in the nanoscale relative surface friction of POSS/polypropylene and POSS/nylon6 HPNC's.[4] The goal of the present study is to evaluate and understand the macroscale surface friction response of POSS/polypropylene HPNCs in relation to POSS concentration, humidity, and external applied load.

Experimental

Materials. Polypropylene (PP) homopolymer (Hival® 2420) was purchased from General Polymers and octaisobutyl POSS (Oib-POSS, Figure 3) was provided by Hybrid Plastics Inc.

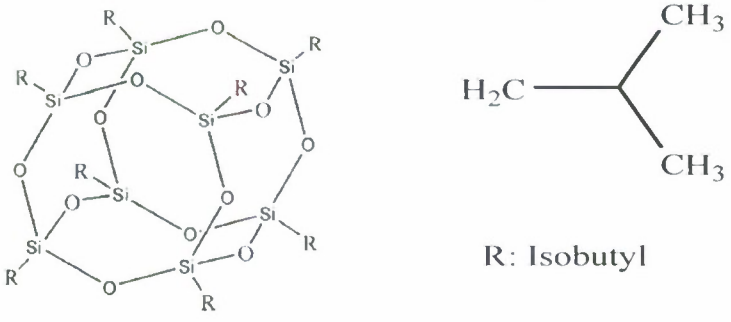

Figure 3. Structure of Oib-POSS molecule with corner isobutyl groups.

Sample Preparation. Oib-POSS/PP nanocomposites were prepared by mixing 0, 5, and 10 weight% crystalline Oib-POSS powder into PP matrix at 225°C and 300 rpm utilizing CT-25 co-rotating twin screw extruder (B&P Processing, screw diameter = 25 mm and L: D ratio of 40:1). Smooth films for relative surface friction studies were prepared by melt pressing the nanocomposite samples.

Macroscale Friction Measurements. Dynamic coefficient of friction (COF) measurements were performed according to ASTM G 99, using a pin-on-disk tribometer (Micro Photonics Inc., PA). Two sets of readings were taken for each film sample (1" x 1") inside a controlled humidity chamber at 27°C. Film samples were mounted firmly on a flat metal disc, which was rotated (path radius 3 mm) against a steel ball (3 mm diameter, Small Parts Inc., Miami Lakes, FL) at 20 rpm for 20 min. Relative friction measurements were conducted as a function of relative humidity (15%, 60%, and 90% RH at 3N external load) and external load (3N, 4N, and 5N at 60% RH).

Results and Discussion

Response to Humidity. Variation in the relative surfaee friction of Oib-POSS/PP HPNCs as a function of POSS concentration at 15%, 60%, and 90% relative humidity and an external load of 3 N are shown in Figure 4. Oib-POSS/PP HPNCs exhibit lower relative friction compared to neat PP at all three humidity levels (dry to highly humid). On an average, relative surface friction reduced by 21%-71% upon incorporation of 5% and 10% Oib-POSS in PP, respectively. This effect is attributed to the presence of uniform, spherical nanoscopic POSS molecules on the film surface that exhibit lower friction levels than PP. Additionally, lower friction values were noted at higher humidity levels. For example, the 10% Oib-POSS/PP sample exhibited an increase in surface friction reduction from 65% to 77% as humidity changed from 15% to 90%. This effect can be explained in part due to the presence of a thin moisture layer on the film surface, which acts as a lubricant and reduces the relative surface friction.

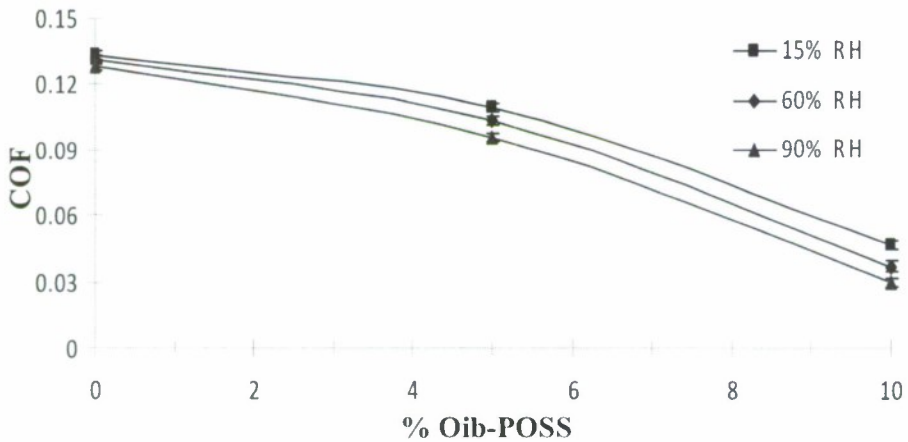

Figure 4. COF as a function of POSS concentration at different humidity.

Response to External Load. Variation in the relative surface friction of Oib-POSS/PP HPNCs in relation to the POSS concentration at different external loads of 3N, 4N, and 5N at 60% relative humidity are shown in **Figure 5**. All samples exhibited higher surface friction with increase in external applied load. However, Oib-POSS/PP HPNCs exhibit lower relative friction compared to neat PP at all the three loads.

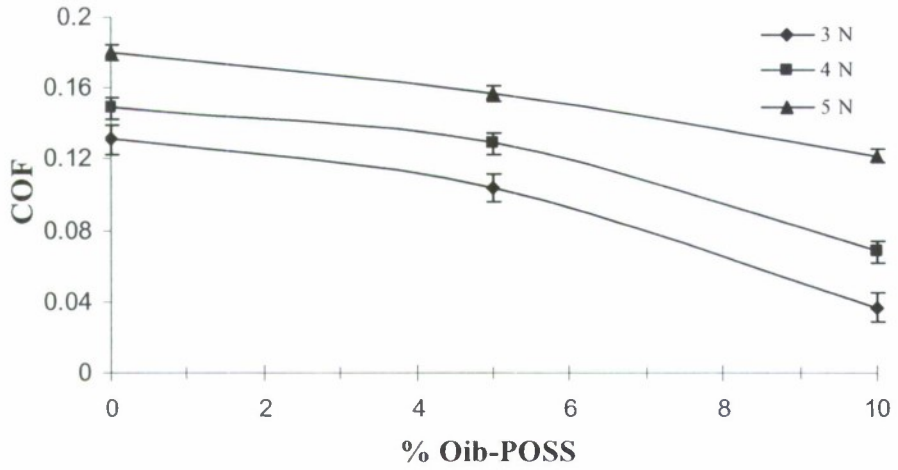

Figure 5. COF as a function of POSS concentration at different loads.

Conclusions

Oib-POSS/PP HPNCs with POSS enriched surfaces were successfully prepared by melt blending via twin screw extrusion. A pin-on-disk tribometer was utilized to study the relative friction response of Oib-POSS/PP HPNCs in relation to the POSS concentration, humidity, and external load. Incorporation of Oib-POSS in the PP matrix led to a reduction in macroscale relative surface friction, while increasing POSS concentration resulted in decreasing relative surface friction. On average, the nanocomposite sample with 10% Oib-POSS showed a 71% reduction in surface friction compared to the neat PP surface. In our previous studies on similar HPNC systems, similar trends were reported at nanoscale relative surface friction measurements *via* lateral force microscopy.

---

1 Misra, R.; Rollins, K.; Morgan, S. E. "Low friction polyhedral oligomeric silsesquioxane (POSS)/polypropylene hybrid nanocomposites" Polymer Preprints (American Chemical Society, Division of Polymer Chemistry) **(2008)**, 49(1), 517-518.

2 Lichtenhan, J. D.; Schwab, J. J.; Reinerth, W. A. "Nanostructured Chemicals: A New Era in Chemical Technology," *Chemical Innovation* **2001**, 3-5.

3 Lichtenhan, J.D.; Noel, C.J.; Bolf, A.G.; Ruth P.N. *Mat. Res. Soc. Symp. Proc.*, **1996**, 435, 3.

4 Misra, R.; Fu, B.; Morgan, S. E. *J Polym Sci Part B: Polym Phys* **2007**, *45*, 2441-2455.

HIGH OXYGEN BARRIER MATERIALS BASED ON HYPERBRANCHED ALIPHATIC POLYESTERS CONTAINING MULTIPLE HYDROXYL GROUPS

PI: Sergei Nazarenko

Summary

This work explored commercially available Boltorn™ dendritic hydroxylated aliphatic esters to provide a new material platform for development of high oxygen barrier biodegradable films and coatings. Improved mechanical behavior was achieved via covalent linking of dendritic molecules using 1,6-hexamethylene diisocyanate. This report encompasses the information on structure, thermal, mechanical, oxygen barrier, and biodegradation behavior of pure and network systems.

Introduction

The recognized lack of biodegradability of most commercial polymers, in particular those used for food packaging, focused public attention on the potential global environmental problem associated with plastic waste build-up in the countryside and on the seashore. Therefore, there is a growing demand for sea-biodegradable polymers.

Biodegradability is promoted by enzymes and it is generally accepted that only some hetero-chain polymers, i.e., aliphatic polyesters are truly biodegradable, although in practice the bio-assimilation step normally proceeds first via abiotic hydrolysis which results in monomeric and oligomeric products that are more readily consumed by microorganisms in the environment (*1-3*). While most commercially available biodegradable synthetic polyesters used for food packaging applications today, for instance poly(lactic acid) (PLA), polycaprolactone (PCL), poly(3-hydroxybutyrate-co-3-hydroxyvalerate) (PHBV) etc., have reasonably good water barrier, they unfortunately exhibit a mediocre oxygen barrier which is not high enough to satisfy the current market for packaging of oxygen-sensitive food (*4, 5*). The oxygen permeability of these biodegradable polyesters is somewhat comparable or in most instances higher than that exhibited by poly(ethylene terephthalate) (PET). A search for new biodegradable aliphatic esters with more advanced properties, in particular oxygen barrier, is ongoing.

Dendritic macromolecules exhibit compact globular structures which lead to their low viscosity in the melt or in solution. Furthermore, dendritic macromolecules are characterized by a very large number of available functional groups, which lead to unprecedented freedom for changing/tuning/tailoring the properties of these multivalent scaffolds via complete or partial derivatization with other chemical moieties. All these features have contributed to multi-disciplinary applications of these unique macromolecular structures in recent years (*6, 7*). The development of efficient synthetic routes in recent years has given rise to a virtually unlimited supply of commercially available dendritic polymers, at very affordable price. The transport properties of hyperbranched and dendritic polymers have recently attracted attention as potentially new barrier and membrane materials (*8-9*).

Commercially available hyperbranched aliphatic polyesters (Boltorn™ polyols) attracted our attention as potentially very interesting candidates for the aforementioned applications because of their degradable aliphatic ester nature and the presence in the structure of multiple hydroxyl groups which is an important attribute for the polymer to exhibit high oxygen barrier due to hydrogen bonding. The pseudo-one-step, divergent synthesis of these aliphatic-ester dendritic polymers, first described by Malmström *et al.* in 1995, involves sequential addition of monomer during synthesis; each addition corresponds to the stoichiometric amount of the next generation (*10*).

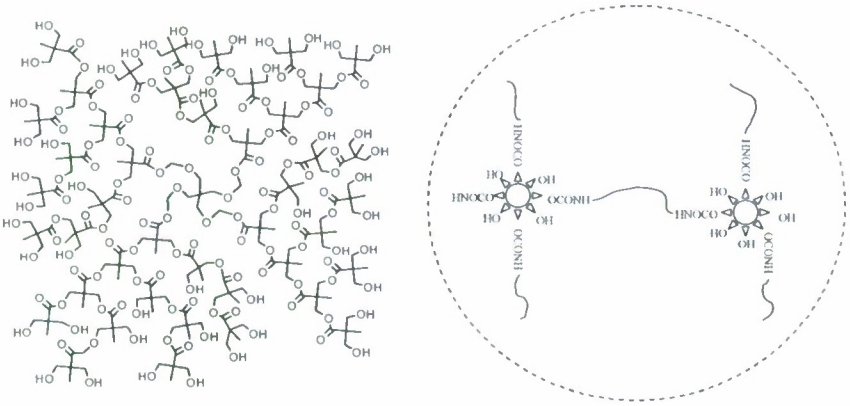

Fig1 Schematics of Boltorn™ hyperbranched aliphatic esters. Insert shows the network formed by covalent linking of hyperbranched moleculeswith diisocyanate.

Although characterized by imperfect branching and significant polydispersity, these polymeric structures preserve the essential features of dendrimers, namely, high end-group functionality and a globular architecture. An imperfect dendrimer structure (4th generation) of hydroxylated polyester based on 2,2-bis-methylopropionic acid (bis-MPA) with an ethoxylated pentaerytriol (PP50) core is shown in Figure 1. Fourth generation Boltorn™ polyols contain 64 hydroxyl groups per molecule. Imperfect branching, which leads to incorporation of linear bis-MPA units, naturally introduces hydroxyl groups not only in the periphery as can be expected in the case of ideal dendrimers but also within the dendritic shell structure.

In contrast to linear polymers, the lack of chain entanglements between dendritic units and the overall globular architecture make dendrimers fairly weak when in the bulk. Thus to make materials based on dendrimers flexible and mechanically strong, the dendritic units must be covalently linked to form a network as shown in the insert in Figure 1. Considering the polyol nature of Boltorn™ polyesters, using diisocyantes for linking dendritic molecules together was a natural step, as it is well known that isocyanates undergo rapid reactions with compounds containing active hydrogen.

Experimental

Hydroxyl-functional dendritic (hyperbranched) polyestera of 2nd and 4th generation, Boltorn® H40 were obtained from Perstorp Specialty Chemicals AB, Sweden, in the form of pellets. About 100 μm thick films were prepared via compression molding at 130°C in a Carver press followed by cooling under pressure by flowing water through the press platens. Prior to molding, as received pellets were dried in vacuum at 55°C for at least 24 hrs.

Boltorn™ H40 dendritic molecules were covalently linked in this work to make a network with aliphatic 1,6-hexamethylene diisocyanate (HDI). The molar NCO/OH ratio was varied for the reactants from 10 to 50% to prepare networks with different degrees of connectivity of dendritic units. The network samples are designated as H40/Z where Z stands for NCO/OH ratio expressed as a percentage. The network formation reaction of H40 with HDI was carried out in N,N-dimethylformamide (DMF) of 99.8% purity at 90°C. No catalyst was added. Isocyanates react readily with moisture to form urea linkages, therefore special precautionary measures were implemented to prevent moisture uptake either by HDI or DMF. Observation of the reaction vessel was maintained over the course of the reaction to monitor the viscosity of the solution. As viscosity of the solution increased to the desired level, suggesting that the gelation point was near, the solution was cast onto a glass plate which was immediately placed into an environmental chamber purged with dry nitrogen, and left at room temperature for 12 hr to complete the reaction and evaporate most of the residual DMF. The resulting film (~0.1 mm thick) was then peeled and further dried in vacuum first for 72 hr at 55°C and then annealed in vacuum at 155°C for one hour in order to remove even small traces of DMF solvent as the boiling temperature of DMF at 1 atm. pressure is 153°C. TGA, DSC and FTIR analysis confirmed that the amount of DMF left in the system after this drying procedure was negligibly small, i.e., well below the detection limit.

Thermal analysis was conducted using TA Instruments DSC Q-100. The calibration was carried out using indium and sapphire standards. Heating and cooling rates of 10°C min^{-1} were used over the studied temperature range.

The density was measured at room temperature using a density gradient column constructed from toluene and carbon tetrachloride. The column was prepared according to ASTM-D 1505 Method B. The column was calibrated with glass floats of known density. The accuracy of density measurements was estimated to be ± 0.001 g/cm^3. Small pieces (~ 25 mm^2) were placed in the column and allowed to equilibrate before the measurements were taken.

Oxygen transport measurements were conducted at 25°C, 0% and 50% relative humidity RH, 1 atm partial oxygen pressure difference using the commercially manufactured diffusion apparatus OX-TRAN® 2/20 (Modern Control Inc.). This apparatus employs a continuous-flow method (ASTM-D 3985-81) to measure oxygen flux, *J(t)*, through polymer films or thin sheets. In order to obtain the diffusion coefficient and to accurately determine the permeability coefficient, the data, flux, *J(t)*, were fitted to the solution of Fick's second law:

$$\frac{\partial c}{\partial t} = D\frac{\partial^2 c}{\partial x^2} \qquad (1)$$

with boundary conditions for the permeant concentration $c(x = 0, t) = Sp$; $c(x = l, t) = 0$, where S is the solubility coefficient, p is the gas pressure, l is the sample thickness and initial conditions $c(x, t = 0) = 0$:

$$J(t) = \frac{Pp}{l}[1 + 2\sum_{n=1}^{\infty}(-1)^n \exp(-D\pi^2 n^2 t / l^2)] \qquad (2)$$

Permeability, P, and diffusion coefficient, D, were obtained by performing a two-parameter least squares fit of the experimental flux data to equation (2). The solubility, S, was obtained from the relationship $P = D.S.$ The methodology of these oxygen barrier measurements, data analysis, and the sources of experimental error were previously described in detail elsewhere (*11*).

Standard marine biodegradation measurements were performed using ASTM 6691. In this test, powdered samples of dendritic polyols were placed into a bottle containing an inoculum that was consistent with microorganisms and minerals commonly present in the ocean. Biodegradation testing was carried out at 30°C, and involved measurements of gaseous CO_2 released as a final product of enzymatic degradation. From the amount of CO_2 released the amount of degraded (mineralized) polymer carbon atoms can be directly determined and expressed as a % Mineralization which is calculated as follows:

$$\%Mineralization = \frac{C_{Test} - C_{Blank}}{C_{Intial}} \cdot \% \qquad (3)$$

where C_{Test} is the number of biogas carbon atoms produced in the test reactor in the presence of a polymer, C_{Blank} is the number of biogas carbon atoms produced in the reactor without a sample and associated with the bacterial activity present in incubator alone without a polymer, and $C_{Initial}$ is the total number of carbons in polymer sample before degradation.

Biodegradation Behavior

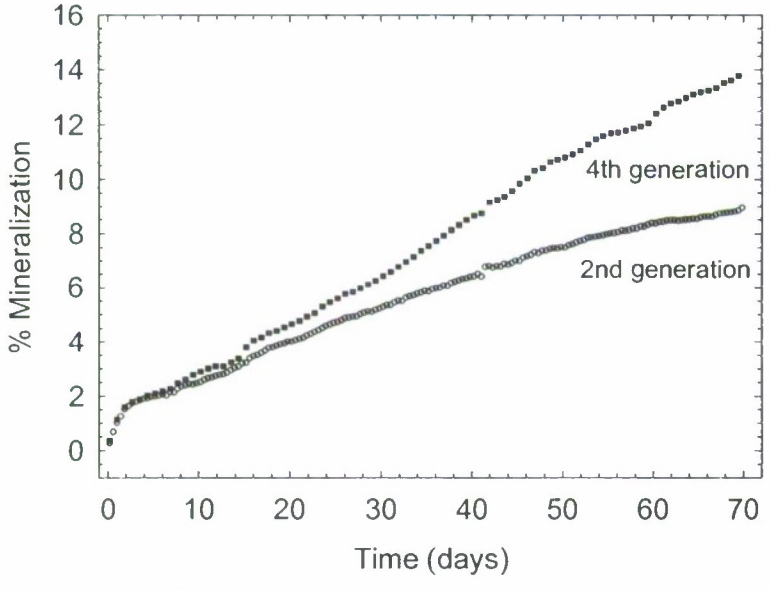

Fig 2 Marine biodegradation behavior of 2nd and 4th Generations of pure Boltorn™ hyperbranched aliphatic esters.

Figure 2 shows preliminary sea biodegradation data conducted on pure 4th and 2nd generations of Boltorm™ dendritic polyols. The figure shows % of mineralization versus time for 4th (curve 1) and 2nd (curve 2) pseudo-generations of pure Boltorm™ dendritic polyols. The marine biodegradation test was conducted for 70 days and by the end of this experiment 14% of H40 carbon and 9% of H20 carbon were converted into CO_2 biogas. This level of mineralization is below that for which Boltorn polyols can be considered truly marine

biodegradable, according to ASTM 7081. Both H40 and H20, except for a fairly short induction time, displayed fairly constant rates of biodegradation at about 0.20%/day and 0.13%/day, respectively. The larger degradation rate of H40 as compared to H20, by about 1.6 times, was attributed to a larger weight concentration of ester groups for this generation (1.5 times that of H20). The corresponding weight concentrations of ester groups were calculated based on the experimentally determined molecular weights M_w, as reported by Perstorp, for 2nd and 4th generations, 1800 and 5900 g/mol, and ester groups per molecule, 12 and 60, correspondingly.

Polymers do not normally biodegrade until they are broken down into fairly low molecular weight chemical species that can be assimilated by microorganisms. Aliphatic polyesters degrade in the presence of water by sequential hydrolytic cleavage of the backbone ester bonds leading to production of monomeric hydroxyl carboxylic acids which in turn can be metabolized by bacteria (*3*).

The hydrolytic degradation proceeds either at the surface (homogeneous) or within the bulk (heterogeneous). The observed zero-order degradation kinetics for H40 and H20 samples suggested homogeneous (surface) mechanism of hydrolysis of pure Boltorn™ dendritic polyols followed by biotic assimilation of water soluble low molecular products of the hydrolysis. It is widely accepted that the surface abiotic degradation is considerably slower than the bulk one. A question can be posed; why surface hydrolysis dominated over bulk degradation in the case of pure dendritic polyols? One of the factors, experimentally confirmed in this work by DSC, was that the absorbed water in pure Boltorn™ polyols is formed predominantly in the unbound state, capable of freezing upon cooling. The unbound water seems to be much less hydrolytically reactive as compared to bound water, as the later is typically bonded to polar groups, in particular to the hydrolytically unstable ester groups. In turn, we determined that the absorbed water in crosslinked dendritic polyols formed predominantly in the bound state associated with the urethane networks, especially for NCO/OH concentration above 20%. Therefore, we anticipated that the networks may exhibit a different abiotic degradation behavior as compared to pure polyols.

As sea biodegradation investigation of cross-linked dendritic polyols is under scrutiny at Natick, tests were conducted to compare abiotic (hydrolysis) degradation of pure H40 Boltorn® and H40 cross-linked with HDI (NCO/OH=35%). The film samples under comparison were placed in the buffer aqueous solution at 37°C. The wet weight was periodically measured. The mass uptake kinetics of the cross-linked sample are shown in Figure 3, with the cross indicating the point at which the sample disintegrated completely, only a few tiny particles were present in the solution.

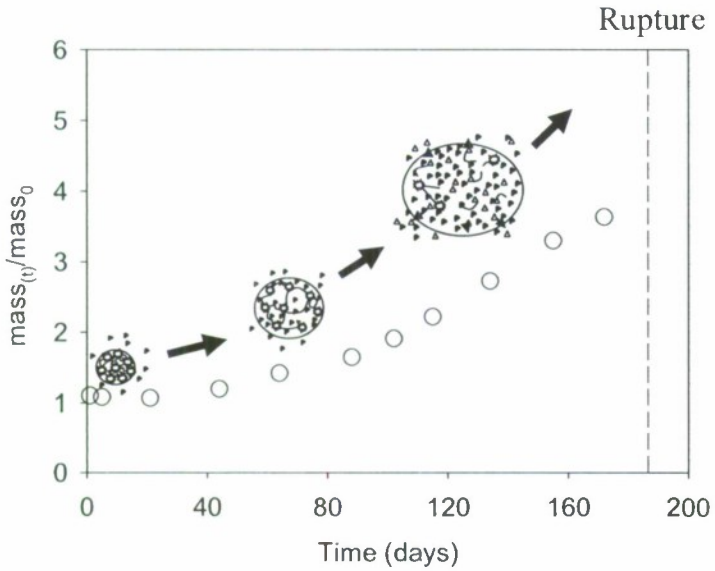

Fig 3. Water uptake behavior associated with abiotic degradation of Boltorn ™H40/HDI (NCO/OH=50%) network.

The interesting observed feature of cross-linked samples is that they easily formed a hydrogel in the buffer solution while H40 remained essentially unswelled. The wet weight of swelled cross-linked samples increased exponentially with time, indicative of the decreased cross-linking density due to the hydrolysis reaction in the bulk. Eventually, the highly swelled cross-link sample completely disintegrated, practically overnight, ("exploded") after being exposed to the aqueous environment for about 6 months. At about the point of rupture, "explosion", the dry weight was found to be 28% of the original, so 72% percent of the polymer has been hydrolyzed to small monomer or oligomer produets and dissolved in water. Interestingly, in the same experiment the sample of pure H40 degraded in the aqueous environment much slower as compared to the cross-linked one. Large pieces of H40 were still present in aqueous solution after the cross-linked sample completely disintegrated. The difference in the rate of abiotic degradation between pure and cross-linked H40 was attributed to the fact that first degraded via a surface, and the second via a bulk degradation mechanism.

Thermal and Stress Behavior

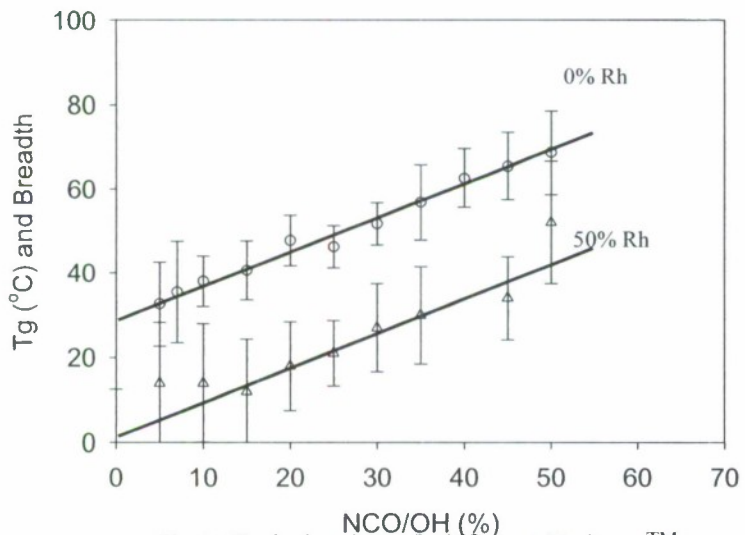

Fig4. Tg behavior of different Boltorn™ H40/HDI networks at 0% and 50% RH

Dendritic polymers are multivalent scaffolds, so the possibility that one HDI molecule reacts with two hydroxyl groups of the same dendritic unit can not be completely ruled out. Intra-molecular cross-links, associated with formation of loops, are not as efficient as inter-molecular cross-links, and typically lead to leveling off the glass transition temperature. To explore this behavior the dependence of Tg versus NCO/OH ratio was measured at 0 and 50% RH by DSC. Figure 4 displays Tgs as a function of NCO/OH ratio with the breadth of the transition shown as error bars.

Tgs at 0%RH were determined using the second scans, while first scans were used to determine Tg at 50% RH for samples specifically conditioned at these levels of relative humidity prior to testing. Tg gradually increased from about 20°C to 70°C upon changing NCO/OH ratio from 0 to 50%. This result is in clear support of the predominant formation of intermolecular cross-links. Humidity played a pivotal role in lowering Tg due to breaking of the existing hydrogen bonding network and plasticizing the network structure. At 50% RH, Tgs increased from about 0°C for pure H40 to about 50°C for cross-linked samples with NCO/OH = 50%. Two Tg trends at 0 and 50% RH are almost shifted in parallel fashion relative to each other, with a shift factor of about 20 degrees.

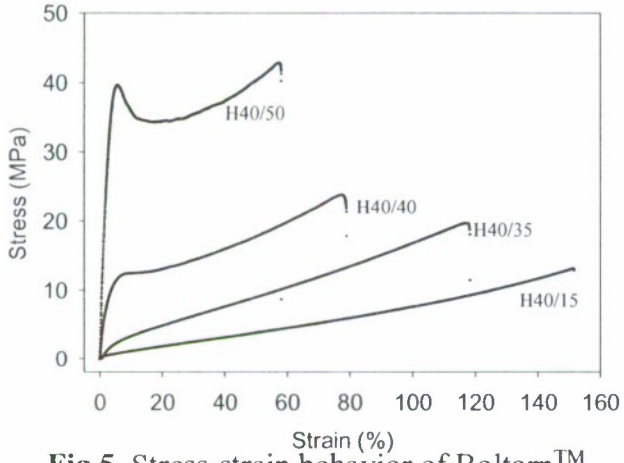

Fig 5. Stress-strain behavior of Boltorn™ H40/HDI networks.

Engineering stress-strain curves of cross-linked samples are shown in Figure 5. All cross-linking materials showed dramatic improvement of mechanical properties at ambient conditions (RT and 50%RH) as compared to films made of pure H40 which were very brittle. Stress-strain behavior for samples with NCO/OH up to 35% was similar to that typically reported for the rubbery state, while beyond 35% a clear transition to the glassy state stress- strain behavior characterized by a much higher Young's modulus, yield point and a strain softening was apparent. Naturally, samples in the rubbery state exhibited larger elongation at break. Sample with NCO/OH=15%, for instance, exhibited elongation at break ε_b =150% and sample with NCO/OH =35% the elongation at break was ε_b=110%. The residual deformation of these samples recovered completely within a few minutes after unloading for these samples. Samples in the glassy state exhibited smaller elongation at break, however, it was still quite impressive; e.g. a sample with NCO/OH ratio 50% had ε_b=55%.

Oxygen Barrier Behavior

Oxygen barrier data for pure H40 systems and H40 network systems measured at RT and 0 and 50%RH are summarized in Table 1 which also reports Tg's and densities in the dry state. Due to the high concentration of hydroxyl functional groups in the periphery, excellent gas barrier characteristics for pure H40 are predicted. As seen in Table 1, the pure H40 at 0%RH displayed considerably better oxygen barrier characteristics than PET and comparable to those for EVOH with 48% (mol/mol) of ethylene. EVOH copolymers with low and moderate ethylene content are considered benchmark materials for packaging applications. When exposed to ambient humidity (50% RH) the barrier properties were reduced, but still better than PET. Figure 6 (a), (b), and (c) also shows the corresponding graphs of permeability, diffusivity and solubility as a function of NCO/OH ratio determined at 0 and 50% RH.

Table 1: Oxygen barrier characteristies of pure Boltorn™ H40 and H40/HDI networks at 0 and 50% RH.

Materials	T_g (°C)	Density (g/cm^3)	Rh (%)	P	D	S
H40/0	23.3	1.2832	0	0.91	2.7	3.9
	-1.0	-	50	7.70	35.8	2.5
H40/10	38.1	1.2813	0	1.60	6.9	2.7
	14.0	-	50	6.30	36.0	2.1
H40/20	47.7	1.2703	0	1.30	9.4	1.6
	18.0	-	50	5.63	33.9	1.9
H40/35	56.8	1.2609	0	3.06	8.8	4.0
	30.0	-	50	2.60	14.3	2.2
H40/50	68.6	1.2449	0	6.40	13.0	7.7
	52.0	-	50	5.60	18.7	3.5
*PET	76	1.3370	0	39.30	56.0	9.8
	-	-	50	-	-	-
*EVOH48	48.0	1.1200	0	0.97	4.16	2.1
	-	-	50	-	-	-

*Measurements performed in authors lab.
P – [10^{-2} cc(STP) cm m^{-2} day^{-1} atm^{-1}].
D – [10^{-10} cm^2 s^{-1}].
S – [10^{-2} cc(STP) cm^{-3} atm^{-1}].

Because $P = D \cdot S$, an understanding of D and S trends beside P was essential to draw a complete picture of transport behavior. At 0%RH oxygen permeability exhibited a gradual inerease from P = 0.009 ee-em/m^2-day-atm for pure H40 to P = 0.064 ee-em/m^2-day-atm for H40 with NCO/OH = 50%. In the case of NCO/OH =35% P = 0.031 cc-cm/m^2-day-atm. Therefore praetieally speaking, oxygen barrier of dry cross-linked films was not that different from that displayed by pure H40. Both oxygen diffusivity and solubility exhibited a gradual increase with cross-linking as free volume inereased (density deereased) with Tg as ean be seen from Table 1. Thc cffect of Tg on development of excess hole free volume and increase of gas transport charaeteristies has been deseribed in details elsewhere (*12, 13*). Changes in diffusivity controlled thc permeability predominantly at smaller NCO/OH ratios and changes in solubility controllcd it at larger NCO/OH ratios. At 50% RH, oxygen gas barrier properties cxhibited a more eomplex trend. This trend was due to the transition from the rubbery to glassy state, cxhibited by eross-linked polyols at RT and 50%RH. This effeet is somewhat similar to that diseussed in the previous section with regards to stress-strain behavior, also determined at 50% RH. At 50%RH pure H40 displayed the largcst oxygen permeability (worst barrier) P = 0.078

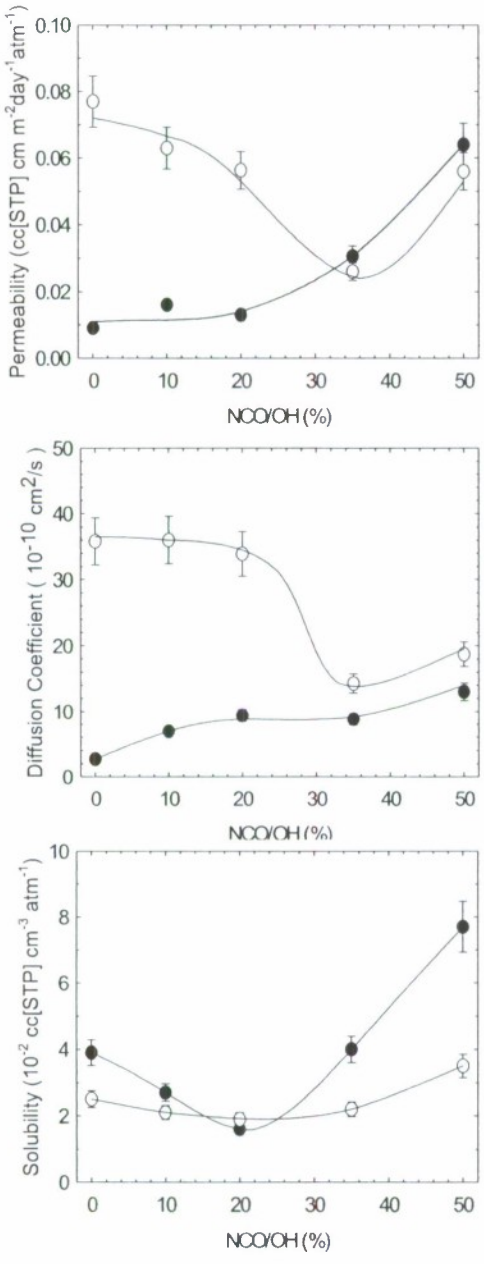

Fig 6. Oxygen Permeability, Diffusivity and Solubility of H40/HDI networks. Filled symbols are data at 0%RH and opened symbols are data at 50%RH.

cc-cm/m^2-day-atm which was 8.5 times larger than that displayed by dry H40. With an inereasing ratio of NCO/OH, oxygen permeability gradually deereased to P = 0.026 cc-cm/m^2-day-atm, reaching this minimum at NCO/OH ratio of about 35%, then permeability increased again. For a sample with NCO/OH = 50% P = 0.056 cc-cm/m^2-day-atm. Therefore cross-linked polyols with NCO/OH ratio in the range of 30-40% in addition to excellent mechanical properties exhibited reasonably high oxygen barrier at 50%RH, although not as good as pure H40 at 0%RH. Oxygen permeability of the system with NCO/OH =35% at 50% RH was almost 3 times smaller than that for pure H40 at the same RH. Therefore, oxygen barrier of pure H40 at 50%RH was improved via cross-linking with HDI. At lower NCO/OH ratios, oxygen permeability for cross-linked systems was controlled by solubility, which deereased more gradually. Oxygen diffusivity changed very little, until about NCO/OH =20%. Then diffusivity, in contrast to solubility, upon transition from rubbery to the glassy state deereased by almost a factor of 4 predominantly determining oxygen permeability trends in the range NCO/OH 20-35%. Above NCO/OH= 35%, again oxygen solubility was determining oxygen permeability behavior as in this range of cross-linking oxygen diffusivity exhibited relatively small change.

Conclusions

This work explored the potential of commercially available Boltorn™ dendritic hydroxylated esters as high oxygen barrier biodegradable films and coatings. Improved mechanical performance was achieved via covalent linking of dendritic molecules with 1,6-hexamethylene

diisocyanate. Oxygen transport for both the pure and cross-linked dry (0%RH) polymer films exhibited excellent oxygen barrier properties, considerably better than PET and comparable to that for EVOH with 48% (mol/mol) of ethylene. At 50% RH, the oxygen barrier of pure dendritic polyols was reduced. Hydrogen bonding was found to play a major role in determining the oxygen barrier and water sensitivity of these polymers. Cross-linked materials at 0% RH exhibited a gradual increase in oxygen permeability (reduction of barrier) as compared to dendritic polyols. This behavior was attributed to the increase of Tg and free volume of the films with the degree of cross-linking. A more complex trend developed when the oxygen permeability was examined at 50% RH due to the transition from the rubbery to glassy state, exhibited by cross-linked polyols at RT and 50%RH. The benefit of this transition is the improvement of oxygen barrier of cross-linked systems over the pure polymer. Biodegradation measurements of pure Boltorn dendritic hydroxylated polyesters showed that they degrade, however, at a rate too slow for them to be considered truly marine biodegradable. Also, cross-linking with HDI resulted in a peculiar acceleration

References

1. Hammond, T.; Liggat, J. J. *Degradable Plastics*; Scott, G.; Gilead, D. (Eds.) Chapman and Hall: NY, **1995**, pp 88-101.
2. Tokiwa, Y.; Ando, T.; Suziki, T.; Takeda, K. " *Biodegradation of Synthetic Polymers Containing Ester Bonds*," in Agricultural and Synthetic Polymers, Biodegradability and Utilization; Glass, J. E.; Swift, G. (Eds.) ACS Symposium Series 433; ACS: Washington, DC **1990.**
3. *Degradable Aliphatic Polyesters*; Albertson, A-C., Ed.; Advances in Polymer Science 157; Springer-Verlag, Berlin, **2001.**
4. *Bio-based Packaging Materials for the Food Industry: Status and Perspectives*; Weber, C. J., Ed.; Department of Dairy and Food Science, The Royal Veterinary and Agricultural University: Denmark, **2000.**
5. Cava, C.; Gimenez, E.; Gavara, R.; Lagaon, J. M. *J. Plastic Film Sheeting* **2006**, *22*, 265-273.
6. Bosman, A. W.; Janssen, H. M.; Meijer, E. W. *Chem. Rev.* **1999**, *99*, 1665.
7. Seiler, M. *Chem. Eng. Tech.* **2002**, *25*, 237.
8. Hedenqvist, M. S.; Yousefi, R.; Malmström, E.; Johansson, M.; Hult, A.; Gedde, U. W.; Trollsas, M.; Hedriek, J. L. H. *Polymer* **2000**, *41*, 1827.
9. Lange, J.; Stenroos, E.; Johansson, M.; Malmström, E. *Polymer*, **2001**, *42*, 7403.
10 Malmström, E.; Johansson, M.; Hult, A. *Macromolecules* **1995**, *28*, 1698.
11. Sekelik, D. J.; Stepanov, E. V.; Nazarenko, S.; Schiraldi, D.; Hiltner, A.; Baer, E. *J Polym Sci Part B: Polym Phys.* **1999**, *37*, 847.
12. Vrentas J. S.; Duda, J. L. *J. Appl. Poly. Sci.* **1978,** *22*, 2325.
13. Petropoulos, J. H. *J. Membr. Sci.* **1990**, *53*, 229.

Publications and Presentations

J. D. Pratt, B. G. Olson, J. P. Brandt, M.K. Hassan, J. Ratto, J. S. Wiggins, J. W. Rawlins, and S. Nazarenko, "High Oxygen Barrier Materials Based on Hyperbranched Aliphatic Polyesters",

in *ACS Symposium Series 1004: Trends in Polymer Degradation and Performance*, Edited by M. Cclina, J.S. Wiggins, N. Billingham, Chapter 2, 17-30, 2009

S. Nazarenko, J. Pratt, M. Kaushik, Nanostructured Networks based on Hyperbranched Aliphatic Polyesters, *6th International Symposium on Molecular Order and Mobility in Polymer Systems*, St. Petersburg, Russia, June 2008

J. Pratt, B.G. Olson, J. Brandt, M. Hassan, S. Nazarenko, Novel High Barrier Films Based on Dendritic Polyesters Cross-linked with Hexamethylene Diisocyanate, *2nd International Symposium on Stimuli-Responsive Materials*, The University of Southern Mississippi, Hattiesburg MS, October 2007

J. Pratt, B. G. Olson, S. Nazarenko, Films and Coatings based on Dendritic Polyesters Cross-linked with Hexamethylene Diisocyanate, *34th Annual Waterborn Symposium, Advances in Intelligent Coatings Design*, New Orleans, February 2007

J. Pratt, B.G. Olson, M.K. Hassan, W.L. Jarrett, J.S. Wiggins, J.W. Rawlins, S. Nazarenko, Biodegradable, High Oxygen Barrier Films based on Polyhydroxylated Dendritic Polymers Cross-linked with 1,6-Hexamethylene Diisocyanate, Polymer Preprints (POLY) 48(1), 556-557 *233rd ACS Annual Meeting*, Chicago IL, March 2007

J. Pratt, S. Nazarenko, Novel Biodegradable Films Based On Cross-linked Dendritic Aliphatic Polyesters Containing Multi-functional Hydroxyl Groups, Gordon Conference on Coatings and Films, New London NH, July 2005

S. Nazarenko, J. Pratt, B. Olson, J. Lin, S. Dong, Structure and Oxygen Barrier of Polyhydroxylated Dendritic Polyols, Annual Technical Conference - Society of Plastics Engineers (2005), 63rd, 2020-2024, Boston MA, May 2005

POLYESTER-POLYURETHANES FOR BIODEGRADABLE FOOD PACKAGING AND PALLET STRETCH WRAP

PIs: Robson F. Storcy, Jeffrey S. Wiggins, and Kenneth A. Mauritz

A large volume of plastie waste is generated aboard U.S. Navy ships at sea, particularly films used for pallet streteh wrap and food paekaging. This waste currently must be stored onboard the ships until port is made, and represents a significant cost in labor and storage spaee. Biodegradable plastics that could be safely and ecologically disposed at sea represent a strategic solution to this problem. Seawater hydrolytic degradation of conventional biodegradable polymers such as poly(L-lactic acid) (PLLA) and poly(glycolic acid), is very slow,[1] but its degradation can be accelerated through the use of copolymers and blends (which decreases crystallinity), and by the inelusion of hydrophilic groups such as carboxylie aeid.

Thermoplastic polyurethanes (TPUs) are versatile polymers ereated through the reaetion of a diisocyanate with a mixture of a ehain-extending diol and/or diamine and a polymeric polyol. TPUs are eharaeterized by a phase separated morphology that exists between the so-ealled hard segments (HS) and soft segments (SS). The HS is the produet of the reaetion of the diisocyanate and chain extender, and the SS is the polyol.[2] The polyol is usually either a polyether or polyester; thus polyurethanes offer the possibility of ineorporating biodegradable polyester ehain elements into a family of polymers whose properties can be readily tuned for a variety of applications, including soft plastic and clastomcric applications for which traditional biodegradable polymers are ill-suited.

In this work, biodegradable TPU elastomers were synthesized as shown in Seheme 1. The approach was to blend degradable poly(D,L-laetide-*co*-glycolide) (PLGA) polyesters at 25 or 50 wt% with eommereially available poly(butylene adipate) (PBA) into the SS. The HS eonsisted of dieyelohexylmethane-4,4'-diisoeyanate (H_{12}MDI) and 1,4-butanediol (BD). The aliphatic diisocyanate was chosen for its favorable toxieity profile. Two 50/50 D,L-lactide/glycolide (mol/mol) polyols were used: BD-PLGA and BHMBA-PLGA. Seheme 2 shows the strueture of PBA and the two PLGA polyesters. BD-PLGA was initiated from 1,4-butanediol whereas BHMBA-PLGA was initiated from bishydroxymethylbutanoic aeid (BHMBA), whieh plaees a pendant earboxylie acid group along the backbone of the polyol, and is predieted to yield an increased rate of water uptake and increased overall rate of degradation of the polyol.[3]

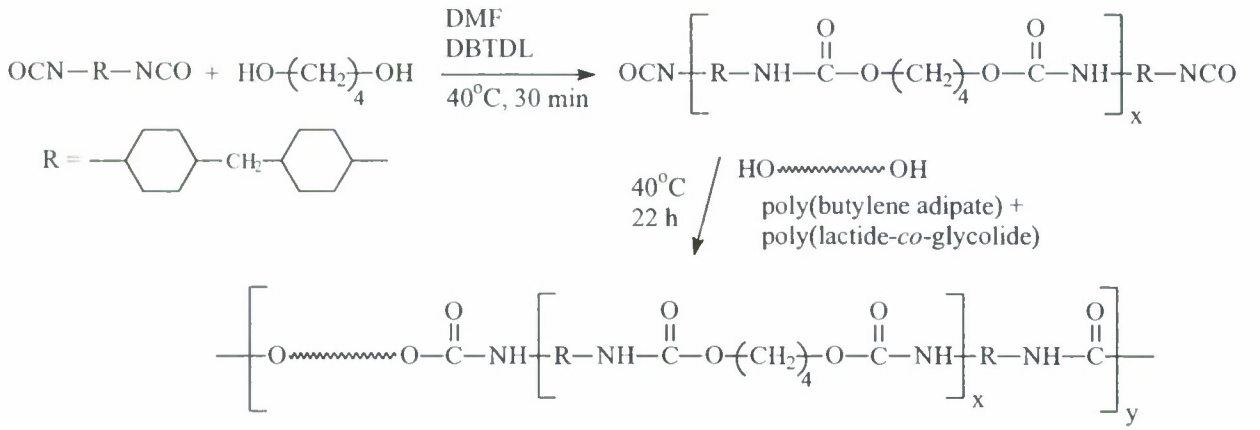

Scheme 1. Synthesis of H_{12}MDI-based TPUs.

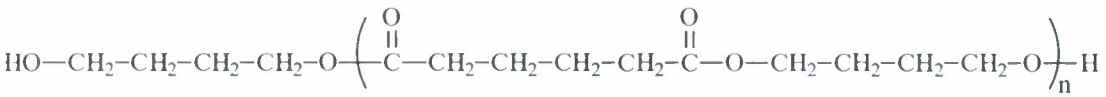

Poly(butylene adipate) (PBA)

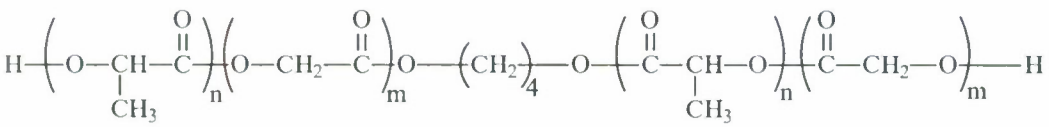

BD-PLGA

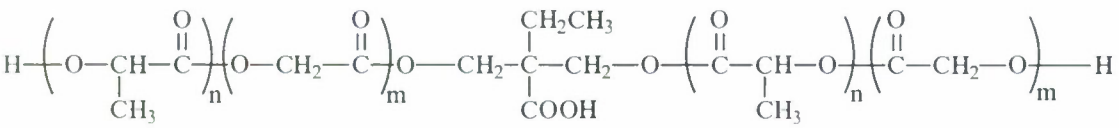

BHMBA-PLGA

Scheme 2. Three polyester polyols used in TPU synthesis.

Table 1 lists the various TPUs that were synthesized. The hard segment content, expressed as the weight ratio of BD to polyol used in the TPU formulation, was set either at 8% or 12% (31.2% or 38.1% hard segment by weight, respectively). In all cases initial [NCO]/[OH] ratio was 1.03. The sample designation used in Table 1 takes the form H-xxx/yy-I, where H is either 8 or 12% HS, xxx is the percentage of PBA polyol, yy is the percentage of PLGA, and I, if applicable, indicates the initiator used to synthesize the PLGA, either BD or BHMBA. As listed in Table 1, the tensile modulus of the TPUs ranged from 9 to 131 MPa and ultimate elongations ranged from 100 to 750%.

Table 1. Performance Data for Degradable TPUs

Entry	TPU	HFIP GPC			Modulus (MPa)	Energy to Break (N*m)	Peak Stress (MPa)	Ultimate Strain	T_g (DMA) (°C)
		M_n (g/mol)	M_w (g/mol)	PDI					
1	8-100/0	33,900	104,1005	3.07	20	8.8	23	7.5	-27
2	8-75/25-BHMBA	12,900	24,100	1.87	15	3.3	10	5.5	5
3	8-75/25-BD	18,400	36,400	1.98	9	3.3	10	6.1	-8
4	8-50/50-BHMBA	8,700	20,500	2.35	131	0.5	7	1.1	5
5	8-50/50-BD	16,200	36,000	2.22	37	1.9	6	4.0	-7
6	12-100/0	71,300	145,900	2.05	13	6.9[a]	20[a]	6.1[a]	-27
7	12-75/25-BHMBA	12,300	29,600	2.42	30	4.8	19	5.2	-
8	12-75/25-BD	11,900	42,600	3.58	27	6.8	22	6.0	-
9	12-50/50-BHMBA	8,100	17,300	2.12	94	2.9	12	3.4	-
10	12-50/50-BD	11,500	35,400	3.09	49	2.8	13	3.5	-

[a] Sample pulled out of grips prior to failure

DMA was used to probe the thermomechanical transitions of the TPUs and indicated useful application temperatures from well below zero up to 60-80°C depending on the formulation. Figure 1 shows DMA results for the 8% HS TPUs. As listed in Table 1, the glass transitions measured by DMA ranged from -27 to 5°C.

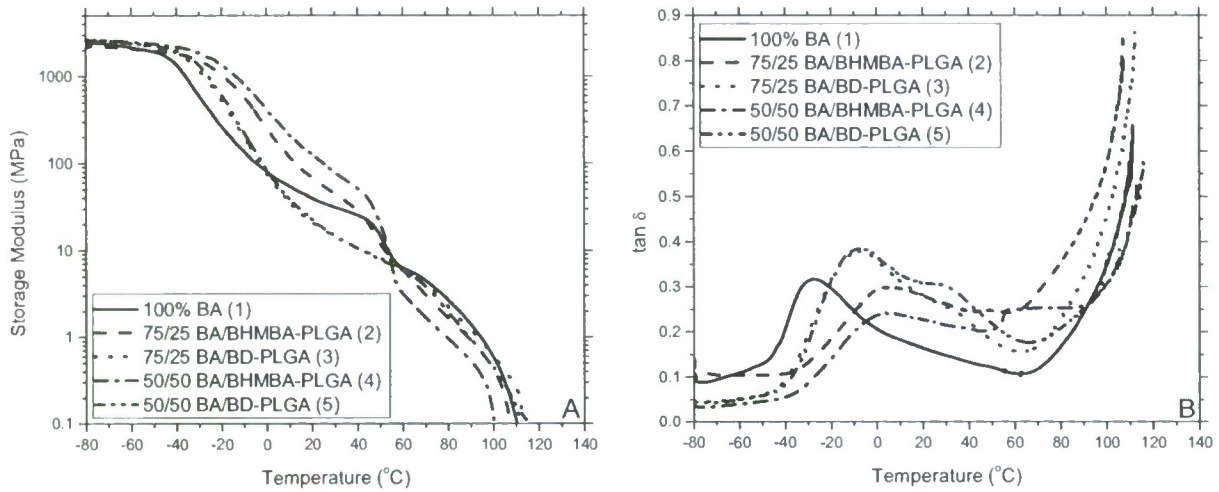

Figure 1. Storage modulus vs. temperature (left) and tan δ vs. temperature (right) for the 8% HS TPUs. The numbers in parentheses correspond to the entry number of Table 1.

Hydrolytie degradation of TPUs was tested in seawater at 37°C (Figure 2). All the PLGA-eontaining TPUs showed enhaneed degradation eompared to those with only PBA as the soft segment. The latter remained essentially unchanged throughout the test while the PLGA-containing TPUs lost as mueh as 45% of their initial mass in 153 days.

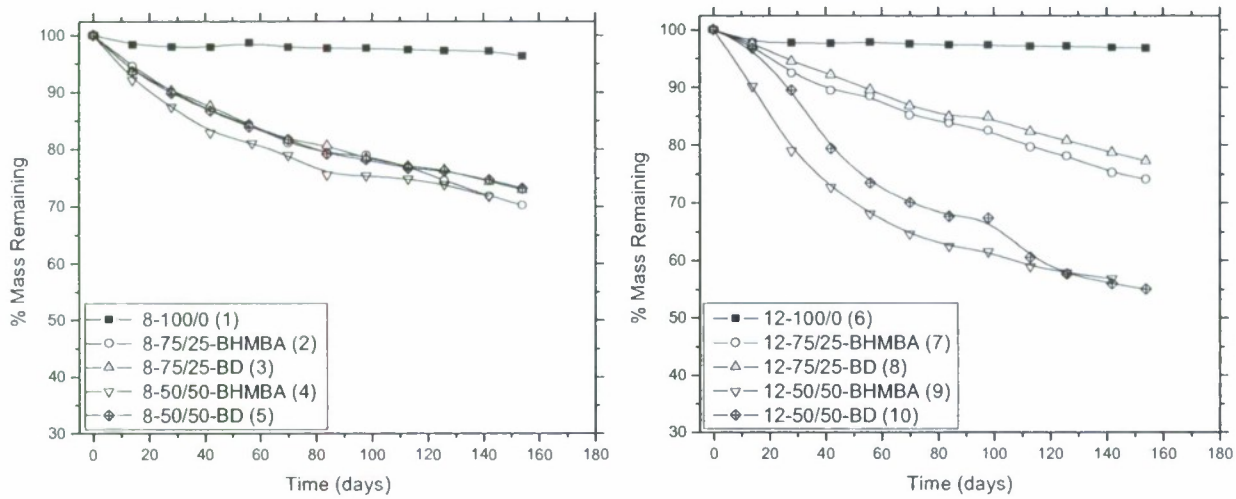

Figure 2. Residual mass of 8% (left) and 12% HS TPUs (right) vs. immersion time in seawater at 37°C. The number in parenthesis corresponds to the entry number of Table 1.

The unique properties of these TPUs make them attractive for food packaging, streteh wrap, and a number of other applieations, even where degradable materials may not have been previously eonsidered. A wide range of properties were obtained by eontrolling the relative amounts of hard and soft segments.

[1] Mayer, J.M.; Kaplan, D.L. *Trends Polym. Sci.* **1994**, *2*(7), 227-235.
[2] Holden, G.; Legge, N.R.; Quirk, R.; Schroder, H.E. *Thermoplastic Elastomers 2nd Edition*; Hanser Publishers: New York, 1996.
[3] Cooper, T.R.; Storey, R.F. *Macromolecules* **2008**, *41*(3), 655-662.

Presentations

Moravek, S.J.; Wiggins, J.S.; Storey, R.F., "Reactive Extrusion of Methyl-2,6-Diisocyantocaproate-Based Degradable Thermoplastic Polyurethanes," 2008 ACS Spring Meeting, New Orleans, LA, March 6-10, 2007.

Moravek, S.J.; Cooper, T.R.; Hassan, M.K.; Wiggins, J.S.; Mauritz, K.A., "Marine-Degradable Thermoplastic Polyurethanes," Symposium on Polymer Performance, Degradation, and Materials Selection, 2007 ACS Spring Meeting, Chicago, IL, March 25-29, 2007.

Moravek, S.J.; Cooper, T.R.; Hassan, M.K.; Wiggins, J.S.; Mauritz, K.A.; Storey, R.F., "Degradable Thermoplastic Polyurethanes Based on 4,4'-Dicyclohexylmethane Diisocyanate," Symposium on Polymer Performance, Degradation, and Materials Selection, 2007 ACS Spring Meeting, Chicago, IL, March 25-29, 2007.

Cooper, T.R.; Hassan, M.K.; Mauritz, K.A.; Storey, R.F., "Synthesis of Poly(D,L-Lactide) Functionalized with Pendant Carboxylic Acid Groups," Symposium on Polymer Performance, Degradation, and Materials Selection, 2007 ACS Spring Meeting, Chicago, IL, March 25-29, 2007.

Publications

1. Moravek, S.J.; Hassan, M.K.; Drake, D.J.; Cooper, T.R.; Wiggins, J.S.; Mauritz, K.A.; Storey, R.F. *in preparation*. "Seawater Degradable Thermoplastic Polyurethanes"
2. Moravek, S.J.; Messman, J.M.; Storey, R.F. *J. Polym. Sci.: Part A: Polym. Chem.* **2009**, *47*, 797-803. "Polymerization Kinetics of *rac*-Lactide Initiated with Alcohol/Stannous Octoate Complexes Using *In Situ* Attenuated Total Reflectance-Fourier Transform Infrared Spectroscopy: An Initiator Study"
3. Moravek, S.J.; Storey, R.F. *J. Appl. Polym. Sci.* **2008**, *109*(5), 3101-3107. "Reaction Kinetics of Dicyclohexylmethane-4,4'-Diisocyanate with 1- and 2-Butanol: a Model Study for Polyurethane Formation"
4. Cooper, T.R.; Storey, R.F. *Macromolecules* **2008**, *41*(3), 655-662. "Poly(lactic acid) and Chain-Extended Poly(lactic acid)-Polyurethane Functionalized with Pendent Carboxylic Acid Groups"
5. Hassan, M.K.; Wiggins, J.S.; Storey, R.F.; Mauritz, K.A. *ACS Symp. Ser.* **2008**, *977*, 153-169. "Broadband Dielectric Spectroscopic Characterization of the Hydrolytic Degradation of Telechelic Poly(D,L-Lactide) Materials"

6. Moravek, S.J.; Wiggins, J.S.; Storey, R.F. *ACS Div. Polym. Chem., Polym. Preprs.* **2008**, *49*(1), 574-575. "Reactive Extrusion of Methyl-2,6-Diisocyantocaproate-Based Degradable Thermoplastic Polyurethanes"
7. Cooper, T.R.; Hassan, M.K.; Mauritz, K.A.; Storey, R.F. *ACS Div. Polym. Chem., Polym. Preprs.* **2007**, *48*(1), 635. "Synthesis of Poly(D,L-Lactide) Functionalized with Pendant Carboxylic Acid Groups"
8. Moravek, S.J.; Cooper, T.R.; Hassan, M.K.; Wiggins, J.S.; Mauritz, K.A.; Storey, R.F. *ACS Div. Polym. Chem., Polym. Preprs.* **2007**, *48*(1), 597. "Marine-Degradable Thermoplastic Polyurethanes"
9. Moravek, S.J.; Cooper, T.R.; Hassan, M.K.; Wiggins, J.S.; Mauritz, K.A.; Storey, R.F. *ACS Div. Polym. Chem., Polym. Preprs.* **2007**, *48*(1), 568. "Degradable Thermoplastic Polyurethanes Based on 4,4'-Dicyclohexylmethane Diisocyanate"
10. Books (as Editor): *Polymer Degradation and Performance*; *ACS Symposium Series #1004;* Editors: M. Celina, N.C. Billingham and J.S. Wiggins; Oxford University Press; American Chemical Society; 2009; ISBN: 978-0-8412-6978-1
11. Broadband dielectric spectroscopic characterization of the hydrolytic degradation of carboxylic acid terminated poly(D,L-lactide) materials; M. Hassan, J.S. Wiggins, R.F. Storey and K.A. Mauritz; Polymer 48 (2007) 2022
12. Biodegradable aliphatic thermoplastic polyurethane based on poly(ε-caprolactone) and L-lysine diisocyanate; M. Hassan, K.A. Mauritz, R.F. Storey and J.S. Wiggins; J. of Poly. Sci.; Part A: Polymer Chemistry 44 (2006) 2990
13. Hydrolytic degradation of poly(D,L-lactide) as a function of end-group: carboxylic acid *vs. hydroxyl*; J.S. Wiggins, M. Hassan, K.A. Mauritz and R.R. Storey; *Polymer*, 47 (2006) 1960
14. *Biodegradable High Oxygen Barrier Films Based on Polyhydroxylated Dendritic Polymers Cross-Linked with 1,6-Hexamethylene Diisocyanate;* J. Pratt, B. Olson, M. Hassan, W. Jarrett, J. Wiggins, J. Rawlins, and S. Nazarenko; *Div. of Polym. Chem., Polym. Preprs.*, 48(1) 2007, 556
15. *Novel method for characterization of poly(D,L-lactide) degradation based on dielectric spectroscopy;* M. Hassan, J. Wiggins, R. Storey, and K. Mauritz; *Polym. Mat. Sci. Eng.*, 51, 2006, 900
16. *L-lysine diisocyanate-based biodegradable thermoplastic polyurethanes with broad range of mechanical properties*; J. Wiggins, M. Hassan, K. Mauritz and R. Storey; *Polym. Mat. Sci. Eng.* 51, 2006, 656

Symposium Organized

Polymer Performance, Degradation, and Material Selection

- American Chemical Society – Division of Polymer Chemistry, National Meeting – Chicago, IL – March 2007
- J.S. Wiggins co-organized with Dr. Mat Celina, Sandia National Labs and Dr. Norman Billingham, University of Sussex, England
- 4 Invited Tutorials, 12 Invited Lectures, 51 Total Professional Presentations

SALT WATER DISPERSIBLE BIODEGRADABLE POLYESTER NANOCOMPOSITES

PI: Lon Mathias

Excellent progress has been made on developing new approaches to nanocomposites and "salt water triggered" dissolution and degradation of polyester composites. We have:

- Prepared nanocomposites based on poly(ε-caprolactone) and organically modified montmorillonite
  - Synthesized a novel imidazolium surfactant having two long alkyl chains one of which contains hydroxyl group as a chain terminal (the product isolated with an excellent yield)
  - Determined the chemical structure of surfactant by NMR spectroscopy
  - Prepared organically modified montmorillonite by ion-exchange reaction between surface bound sodium cations and imidazolium surfactant
  - Determined the amount of organic compound incorporated onto montmorillonite by TGA (the organic content determined as 22 wt%)
  - Revealed intercalation of surfactant between clay platelets by XRD (d-spacing value of pristine montmorillonite increased from 11.8 Å to 18.0 Å upon modification)
  - Prepared nanocomposites by *in situ* intercalative polymerization of ε-caprolactone by using hydroxyl functionality of the surfactant to either react with monomer or polymer
  - Prepared a series of nanocomposites with 1 to 5 wt-% organo-montmorillonite loadings (the inorganic content revealed by TGA was in accordance with targeted amounts)
  - Evaluated polymer formation by NMR and FTIR spectroscopy
- Completed characterization of nanocomposites
  - Recovered polymer chains from the surface of clay platelets by reverse ion-exchange reaction with lithium cations in THF followed by centrifugation
  - Determined molecular weight of polymer by GPC (the molecular weight of PCL chains was controlled by the terminal hydroxyl content; i.e., by the organo-montmorillonite content)
  - Analyzed morphology of nanocomposites by XRD and TEM (the hydroxyl functionality on long alkyl chains had improved ability for grafting of polymer chains from the surface of the clay verified by the highly exfoliated morphology obtained)
  - Evaluated thermal behavior by DSC as well as TGA measurements (highly exfoliated nanostructure does not affect thermal events such as T_m, T_c, T_g, and T_d, the platelets clearly act as nucleating agents for crystallization of PCL matrix and degree of crystallinity increases with clay content)
  - Revealed mechanical properties by DMA (the storage moduli enhanced particularly above T_g, upon increasing the clay content)
- Investigated biodegradation behavior of nanocomposites in marine environment
  - Measured average mineralization of test materials by respirometry experiments

- Compared biodegradation rates of nanocomposites to those of neat polymer (higher rates of degradation were observed for nanocomposites compared to pristine polymer)
- Observed a trend between the addition levels of the organically modified clay and the rate of biodegradation (attributed to highly exfoliated morphology of nanocomposites in which the confinement of polymer chains between the silicate layers is avoided)